EC Journals.ASM.org

Role of the Guanine Nucleotide Exchange Factor Rom2 in Cell Wall Integrity Maintenance of *Aspergillus fumigatus*

Sweta Samantaray, Michael Neubauer, Christoph Helmschrott, Johannes Wagener

Max von Pettenkofer-Institut, Ludwig-Maximilians-Universität, Munich, Germany

***Aspergillus fumigatus* is a mold and the causal agent of invasive aspergillosis, a systemic disease with high lethality. Recently, we identified and functionally characterized three stress sensors implicated in the cell wall integrity (CWI) signaling of this pathogen, namely, Wsc1, Wsc3, and MidA. Here, we functionally characterize Rom2, a guanine nucleotide exchange factor with essential function for the cell wall integrity of *A. fumigatus*. A conditional *rom2* mutant has severe growth defects under repressive conditions and incorporates all phenotypes of the three cell wall integrity sensor mutants, e.g., the echinocandin sensitivity of the Δ*wsc1* mutant and the Congo red, calcofluor white, and heat sensitivity of the Δ*midA* mutant. Rom2 interacts with Rho1 and shows a similar intracellular distribution focused at the hyphal tips. Our results place Rom2 between the cell surface stress sensors Wsc1, Wsc3, MidA, and Rho1 and their downstream effector mitogen-activated protein (MAP) kinase module Bck1-Mkk2-MpkA.**

Aspergillus fumigatus is an airborne opportunistic human pathogen that causes severe invasive diseases in immunocompromised patients. The outcome is often fatal due to limited therapeutic options. All major drugs with activity against *Aspergillus* spp. directly or indirectly attack the fungal cell membrane or cell wall. The fungal cell wall is a conserved structure that mainly consists of chitin, glucans, mannans, and other polymers (1). To overcome cell wall stress, fungi utilize the so-called cell wall integrity (CWI) pathway to adjust the biogenesis of the cell wall. The CWI pathway is a complex signaling network that was best characterized in the baker's yeast *Saccharomyces cerevisiae* (2) (Fig. 1). The CWI pathway encompasses several stress sensors at the cell surface, Rho GTPases, protein kinase C, mitogen-activated protein (MAP) kinases, phosphatases, and other components, and in yeasts, this pathway appears to be roughly conserved (2–4). Cell wall stress is sensed at the cell surface by certain stress sensors. Upon activation, these sensors induce GDP-to-GTP exchange at a Rho GTPase. The activated Rho GTPase transfers the signals to a protein kinase C, which in turn activates a highly conserved MAP kinase module. The final MAP kinase regulates transcription of cell wall-related genes. Notably, the fungal CWI pathway may also comprise other components that may run in parallel to this "classical" pathway or divert from some of the mentioned "classical" effectors. For example, *S. cerevisiae* Rho1 (ScRho1), the Rho GTPase implicated in the CWI pathway, is also known to control polarization of the actin cytoskeleton and thought to control the glucan synthase (*S. cerevisiae* Fks1 [ScFks1]/ScFks2) that synthesizes β-(1,3)-D-glucan, an essential element of the cell wall (2, 5).

Several recent studies focused on the elucidation of the CWI pathway of *Aspergillus* spp. (Fig. 1) and of other molds. We and others have shown that the *Aspergillus* CWI MAP kinase module consisting of the MAP kinase kinase kinase Bck1, the MAP kinase kinase Mkk2, and the MAP kinase MpkA is highly conserved from yeasts to molds (6–9). Several studies suggest the involvement of protein kinase C (PkcA), but direct proof that places PkcA in line with the MAP kinase module in *Aspergillus* spp. is still lacking (10–12). Kwon and colleagues recently characterized five of six Rho GTPases of *Aspergillus niger*, and beside other functional aspects, they found that Rho2 and Rho4 are important to withstand stress caused by chitin binding agents (13). We recently identified and functionally characterized the CWI sensors Wsc1, Wsc3, and MidA of *A. fumigatus*. Wsc1 is specifically required for resistance to caspofungin, a member of the echinocandin antifungal drug class that inhibits β-(1,3)-D-glucan biosynthesis. MidA is specifically required for resistance to the chitin binding agents calcofluor white and Congo red. In addition, we have shown that the Rho GTPases Rho1, Rho2, and Rho4 play a role in CWI maintenance (14). However, the direct involvement of Rho1, Rho2, or Rho4 in the CWI signaling process of *Aspergillus* spp. remains to be demonstrated. Very recently, components of the CWI signaling pathway were also investigated in the filamentous fungus *Neurospora crassa* (15, 16). Overall, it appears that the principal components are also conserved in filamentous fungi; however, the importance of the individual components for fungal physiology, antifungal drug susceptibility, and pathogenicity may differ and have different implications depending on the medical relevance of the organism.

In baker's yeast, the cell wall stress sensors activate ScRho1 through the two guanine nucleotide exchange factors (GEFs) ScRom1 and ScRom2 (2), and in *Schizosaccharomyces pombe*, the two ScRom1/ScRom2-like GEFs *S. pombe* Rgf1 (SpRgf1) and SpRgf2 were also implicated in CWI signaling (17–19). According to these models, these GEFs integrate the initial signals of the diverse known and, potentially, unknown cell wall stress sensors and therefore represent the first common upstream activators of the CWI pathway. On the basis of our recent data, we assumed that a similar signal transduction mechanism might also exist in filamentous fungi, i.e., *A. fumigatus*. We identified one homo-

Received 5 September 2012 **Accepted** 12 December 2012

Published ahead of print 21 December 2012

Address correspondence to Johannes Wagener, johannes.wagener@med.uni-muenchen.de.

doi:10.1128/EC.00246-12

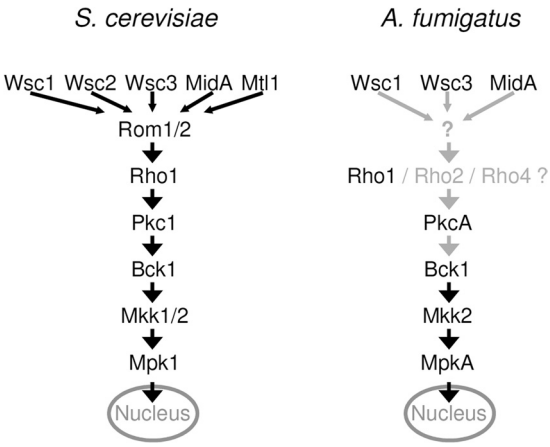

FIG 1 Schemes of the *S. cerevisiae* and *A. fumigatus* cell wall integrity signaling models. Hypothetical signal transduction and components are indicated by gray arrows and proteins.

logue of ScRom1/ScRom2 that we named Rom2. Functional characterization of a conditional *rom2* mutant places Rom2 between the cell surface stress sensors and Rho1 and its downstream effectors.

MATERIALS AND METHODS

Culture conditions and chemicals. The composition of *Aspergillus* minimal medium (AMM) was described previously (20). YG medium contained 0.5% (wt/vol) yeast extract and 2% (wt/vol) D-glucose, and the pH was adjusted to 6.0. For agar plates, medium was supplemented with 2% (wt/vol) agar. Conidia were isolated from cultures on AMM plates that were supplemented with 0.5 μg ml^{-1} doxycycline as required. Potato dextrose agar (catalog no. 213400; Difco) and agar (Bacto agar; catalog no. 214030) were obtained from BD (Franklin Lakes, NJ). Calcofluor white (catalog no. F3543), Congo red (catalog no. 60910), and *trans*,*trans*-farnesol (catalog no. 277541) were obtained from Sigma-Aldrich (St. Louis, MO). Doxycycline (catalog no. 631311) was obtained from Clontech (Mountain View, CA). Yeast extract (catalog no. 103303) was obtained from M.P. Biomedical (Irvine, CA). For transformation, AMM agar plates supplemented with 1.2 M sorbitol were used along with 0.5 μg ml^{-1} doxycycline, 0.1 μg ml^{-1} pyrithiamine (sc-236525; Santa Cruz Biotechnologies, Santa Cruz, CA), and 200 μg ml^{-1} hygromycin B (p21-014; PAA Laboratories, Pasching, Austria) as required.

Strains and plasmid constructions. The nonhomologous end joining-deficient strain AfS35 was used as the wild-type (wt) strain in this study (21). The conditional $rom2_{tetOn}$ strain was constructed essentially as described recently (14). Briefly, the promoter of *rom2* (AFUA_5G08550) was replaced by homologous recombination. To that end, approximately 1 kb of the 5′-flanking region located upstream of the start codon (PCR amplified with primers Rom2-5g08550-5-fwd [fwd stands for forward] and Rom2-5g08550-5-rev [rev stands for reverse]) and approximately 1 kb of the 3′-flanking region that encompasses portions of the *rom2* coding region beginning with the start codon (PCR amplified with primers Prom2-5g08550-5-fwd and Prom2-5g08550-5-rev) were fused to the pyrithiamine-tet-on cassette (acquired by SfiI digestion from pJW123) and transformed in strain AfS35. The C-terminally green fluorescent protein (GFP)-tagged Rom2 ($rom2\text{-}GFP_{gpdA}$) was expressed by cloning *rom2* (PCR amplified with primers Rom2-5g08550-fwd and Rom2-5g08550-fu-rev with chromosomal template DNA) into the PmeI site of pJW103 and transforming the resulting vector pSS001 in strain AfS35. The strain with the inducible expression of $rho1^{G14V}$ ($rho1^{G14V}{}_{tetOn}$) was constructed by transforming pCH003-G14V in AfS35. pCH003-G14V is a derivative of pCH003 that was created by site-directed mutagenesis using the mutagenesis primer Rho1-G14V-SphI and the Change-IT multiple mutation site-directed mutagenesis kit (USB Corporation, Cleveland, OH). pCH003 was constructed by cloning *rho1* (PCR amplified with primers Rho1-6g06900fufnew and Rho1-6g06900-rev with chromosomal template DNA) in pJW121. pJW121 was constructed by cloning the tetracycline-dependent transactivator, the *crgA* terminator, and the *tetO7*::Pmin (a blunt-ended fragment derived from pVG2.2 after digestion with EcoRI and PmeI [22]) into the PmeI site of pSK379. pJW103 and pSK379 were described previously (7, 23). Strains for the doxycycline-inducible expression of the C-terminally 6×His-tagged full-length Rom2 and N-terminally hemagglutinin (HA)-tagged Rom2 with amino acids 733 to 1199 [HA-Rom2(733-1199)] were generated by PCR amplifying full-length Rom2 with primers Rom2-5g08550-fwd and His-Rom2-5g08550-rev and Rom2(733-1199) with the primers HA-Rom2GEF-5g08550-f and Rom2-5g08550-rev and cloning the respective PCR products in pSS005, yielding pSS006 and pSS009. pSS006 and pSS009 were subsequently transformed in strain AfS35. pSS005 is a derivative of pJW121 where the pyrithiamine resistance cassette was exchanged with a hygromycin B resistance cassette. To perform the coimmunoprecipitation experiment, pSS009 [N-terminally HA-tagged Rom2(733-1199)] was transformed in D141 strains constitutively expressing N-terminally GFP-tagged Rho1 or Rho3, which were previously described (7). D141 is the parental wild-type strain of AfS35. Strains encoding the C-terminal GFP-tagged *rom2* at the endogenous locus were constructed by transforming pSS011 in the respective parental strains (AfS35 and $rom2_{tetOn}$ strain), yielding the *rom2-GFP* and $rom2\text{-}GFP_{tetOn}$ strains. pSS011 was cloned by digesting pSS001 with BstBI and pSS005 with BglII followed by blunt ending and further digestion with Acc65I. A pSS001 fragment harboring the coding sequences of GFP and the C-terminal region of Rom2 was ligated to a pSS005 fragment harboring the hygromycin B resistance cassette. For each constructed strain, several clones were isolated (in most cases, ≥3 clones), PCR verified for harboring the expected mutation, and tested for having identical phenotypes under the respective conditions. Primers and strains used in this study are listed in Table 1 and Table 2, respectively.

Growth tests and antifungal drug susceptibility testing. All growth tests were performed on AMM unless specified otherwise. Drop dilution assays were performed in a series of 10-fold dilutions derived from a starting suspension of 5×10^6 conidia ml^{-1}. From these suspensions, aliquots of 3 μl were spotted onto agar plates. Antifungal drug susceptibility testing was performed on AMM. Etest strips were obtained from bioMérieux (Marcy l'Etoile, France).

Colorimetric alkaline phosphatase assay. The colorimetric alkaline phosphatase assay was performed as described previously (24) with slight modifications. Briefly, colonies cultured on solid AMM agar were overlaid with liquid soft agar (1% agar) supplemented with 1 M glycine (pH 10.0), 1 M $MgCl_2$, 250 mM $ZnCl_2$, and 10 mM 5-bromo-4-chloro-3-indolylphosphate and incubated at 48°C. Lysed cells appeared blue within 30 to 45 min, whereas wild-type colonies remained unstained even after 2 h.

Coimmunoprecipitation of GFP-Rho1 with HA-Rom2(733-1199). Conidia of the D141 strain expressing the N-terminally GFP-tagged Rho1 (GFP-Rho1) and harboring the doxycycline-inducible HA-tagged Rom2(733-1199) construct were inoculated in AMM (5×10^5 conidia ml^{-1}) and cultured in a shaker at 37°C. After 24 h, 50 μg ml^{-1} doxycycline was added or not, and the cultures were incubated for another 4 h at 37°C. Mycelium was harvested and washed twice with mycelium washing buffer (50 mM Tris-HCl [pH 7.6], 20 mM NaCl, 1 mM phenylmethylsulfonyl fluoride [PMSF]). Five hundred milligrams of mycelium was added to 0.85 ml lysis buffer (50 mM Tris-HCl [pH 7.6], 20 mM NaCl, 1 mM NaF, 2 mM $MgCl_2$, 1% [vol/vol] Triton X-100, 10% [vol/vol] glycerol, 1× complete EDTA-free protease inhibitor [catalog no. 04693159001; Roche Diagnostics, Risch, Switzerland]) in a Lysing Matrix C tube and extracted with a FastPrep-24 (M.P. Biomedical; Irvine, CA) 10 times at 5.5 m s^{-1} for 40 s. The samples were centrifuged for 15 min at 21,000 × *g* at 4°C, and 2 ml supernatant was added to 20 μl Pierce anti-HA agarose (catalog no.

TABLE 1 Oligonucleotides used in this study

Primer	Sequence
Rom2-5g08550-5-fwd	TTGCGGCCGCTCCTTAGGCGCGTGACGG
Rom2-5g08550-5-rev	CGGGCCATCTAGGCCGCTTCTACCTCTGACAG
Prom2-5g08550-3-fwd	GTGGCCTGAGTGGCCATGGCCGATCTCGGTGGCC
Prom2-5g08550-3-rev	TTGCGGCCGCCGACCCGTGAGAGCAGGGC
Rom2-5g08550-fwd	ATGGCCGATCTCGGTGGCC
Rom2-5g08550-fu-rev	GCCGCCGCTTGTTGTTGTTGGGGCTTGTTC
Rho1-6g06900fufnew	AGGCGGCATGGCTGAAATCCGCCGCAAG
Rho1-6g06900-rev	TTACAAAATAGTGCACTTGCCCTTC
Rho1-G14V-SphI	GTCATCGTTGGCGATGTCGCATGcGGTAAGACTTGTCTTC
His-Rom2-5g08550-rev	TCAGTGGTGGTGGTGGTGGTGGGAGCCGCGGCCGCC TTGTTGTTGTTGGGGCTTGTTC
HA-Rom2GEF-5g08550-f	ATGTACCCATACGATGTTCCAGATTACGCTGCCAGCCTT CACGGCGATG
Rom2-5g08550-rev	TCATTGTTGTTGTTGGGGCTTG

26180; Thermo Fisher Scientific, Rockford, IL) and incubated in an end-over-end mixer at 4°C. After 5 h, the agarose was transferred to a spin column and washed two times with 0.5 ml agarose washing buffer (25 mM Tris-HCl [pH 7.2], 0.15 M NaCl, 1 mM NaF, 2 mM $MgCl_2$, 0.05% [vol/vol] Tween 20, 1× complete EDTA-free protease inhibitor). The agarose was heated at 95°C for 5 min in 25 μl nonreducing sample buffer (catalog no. 26180; Thermo Fisher Scientific, Rockford, IL). The eluate was supplemented with 1.5 μl 2-mercaptoethanol and 1 μl of a 100× complete EDTA-free protease inhibitor stock solution. The supernatant (2.5 μl per lane) and eluate (7.5 μl per lane) were analyzed by SDS-PAGE (12%) and Western blotting and antibodies directed against the HA tag (monoclonal antibody) (catalog no. H9658; Sigma-Aldrich, St. Louis, MO) or GFP (polyclonal antibody, rabbit; a kind gift from Carsten Bornhövd, Munich, Germany).

Preparation of protein extracts and Western blotting. Conidia were inoculated in 10 ml of AMM and cultured in a tube rotator at 37°C. If needed, 100 μg ml^{-1} calcofluor white was added from a 10 mg ml^{-1} stock solution, and the cultures were incubated at 37°C for an additional 30 min. Protein extracts were generated analyzed essentially as described previously (14). Briefly, mycelium was harvested, resuspended in hot Laemmli buffer (95°C; 2% [wt/vol] SDS, 5% [vol/vol] mercaptoethanol, 60 mM Tris-HCl [pH 6.8], 10% [vol/vol] glycerol, 0.02% [wt/vol] bromophenol blue), and extracted with a FastPrep-24 (M.P. Biomedical, Irvine, CA) at 5.5 m s^{-1} for 40 s, followed by heat denaturation at 99°C for 5 min. After SDS-PAGE (12%) and Western blotting, the samples were analyzed with an anti-phospho-p44/42 MAP kinase (MAPK) monoclonal antibody (4370) from Cell Signaling Technologies (Boston, MA) or anti-GFP antibodies (polyclonal, rabbit; a kind gift from Carsten Bornhövd, Munich, Germany). Monoclonal antibodies directed against the mitochondrial manganese superoxide dismutase (MnSOD) (AFUA_4G11580) or aspf22 (AFUA_6G06770) were used as a loading control (kind gifts from Frank Ebel).

Relative quantification of phosphorylated MpkA. Developed Super RX X-ray films (Fujifilm, Tokyo, Japan) were scanned with a GS-800 calibrated densitometer and analyzed with Quantity One 4.5.0 (Bio-Rad, Hercules, CA). The relative signal intensity (percentage of total adjusted volume of all phosphorylated MpkA signals) and respective standard deviations were calculated for each sample.

Sequence analysis, database searches, and bioinformatic tools. The following genome databases were used: the *Aspergillus* genome database (http://aspergillusgenome.org), the *Saccharomyces* Genome Database (http://www.yeastgenome.org), and the Central *Aspergillus* Data Repository (CADRE) (http://www.cadre-genomes.org.uk). Conserved protein sequence signatures were predicted using InterProScan (http://www.ebi.ac.uk/Tools/pfa/iprscan). The Pfam database (http://pfam.sanger.ac.uk) was used to identify Rho GEF domain-containing proteins of *A. fumigatus*. Alignments and phylogenetic trees were generated with MAFFT (http://www.ebi.ac.uk/Tools/msa/mafft/). The phylogenetic tree was visualized with TreeVector (http://supfam.cs.bris.ac.uk/TreeVector/). Identities and similarities of MAFFT alignments were calculated with Sequences Identities And Similarities (SIAS) (http://imed.med.ucm.es/Tools/sias.html).

Microscopic examination of hyphal growth and morphology. The hyphal growth and morphology assay was performed in 24-well plates. In each well, 5×10^3 conidia were inoculated in 1 ml AMM supplemented with the indicated amount of doxycycline. After incubation, the strains were examined with an Axiovert 25 inverted microscope (Carl Zeiss Microimaging, Göttingen, Germany). Images were taken with a Canon EOS 600D camera (Tokyo, Japan).

Fluorescence microscopy. To determine the localization of Rom2-GFP, the strain was cultured in 15 μ-Slide eight-well slides (catalog no.

TABLE 2 *A. fumigatus* strains used in this work

Strain	Relevant genetic modification or plasmid	Parental strain	Reference
AfS35	*akuA::loxP*	D141	21
$rom2_{tetOn}$ strain	$^{p}rom2$::*ptrA-tetOn*	AfS35	This study
$rho1^{G14V}{}_{tetOn}$ strain	pCH003-G14V	AfS35	This study
$rom2\text{-}His_{tetOn}$ strain	pSS006	AfS35	This study
$HA\text{-}rom2(733\text{-}1199)_{tetOn}$ strain	pSS009	AfS35	This study
rom2-GFP strain	pSS011	AfS35	This study
$rom2\text{-}GFP_{tetOn}$ strain	pSS011	$rom2_{tetOn}$ strain	This study
$rom2\text{-}GFP_{gpdA}$ strain	pSS001	AfS35	This study
$GFP\text{-}rho1_{gpdA}$ strain	pJW103-Rho1	D141	7
$GFP\text{-}rho3_{gpdA}$ strain	pJW103-Rho3	D141	7
$GFP\text{-}rho1_{gpdA}$ $HA\text{-}rom2(733\text{-}1199)_{tetOn}$ strain	pSS009	$GFP\text{-}rho1_{gpdA}$ strain	This study
$GFP\text{-}rho3_{gpdA}$ $HA\text{-}rom2(733\text{-}1199)_{tetOn}$ strain	pSS009	$GFP\text{-}rho3_{gpdA}$ strain	This study

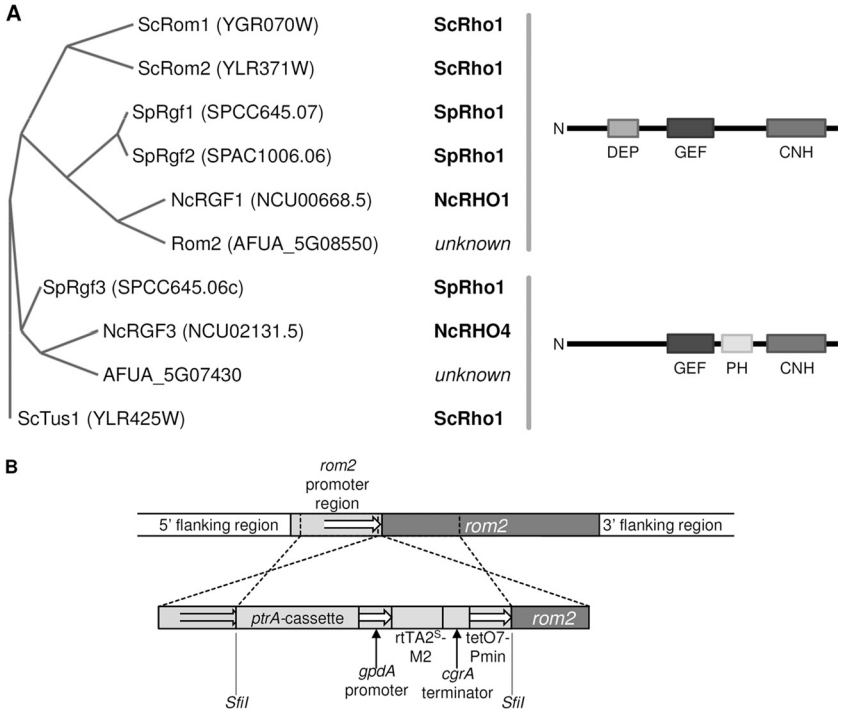

FIG 2 Identification of the putative Rho1 GEF Rom2 in *A. fumigatus* and generation of a conditional *rom2* mutant. (A) Phylogenetic tree of Rho GEF domain (PF00621)-containing proteins of *S. cerevisiae* (Sc), *S. pombe* (Sp), *N. crassa* (Nc), and *A. fumigatus* with similarity to ScRom1/2. The protein sequences of the respective genes were aligned, and the guided tree was generated with MAFFT and visualized with TreeVector. The known interacting Rho GTPases for each GEF and the conserved protein domain structures are listed. (B) The promoter of *rom2* was replaced by homologous recombination with a doxycycline-inducible promoter system. The 5′- and 3′-flanking regions were ligated to the doxycycline-inducible promoter system using the indicated SfiI restriction sites. Respective transformants were isolated and screened for phenotypes and with PCR.

80826; Ibidi, Martinsried, Germany) containing 5×10^2 conidia in 300 μl of AMM in each well. Live cell images were taken after approximately 15 h of incubation at 37°C. Living hyphae were analyzed with a UltraView LCI spinning disc confocal system (PerkinElmer; Waltham, MA) fitted on an Eclipse TE300 microscope (Nikon, Tokyo, Japan) in a temperature-controlled chamber. Images were taken with a black/white ORCA ER camera (Hamamatsu, Hamamatsu City, Japan).

RESULTS

***A. fumigatus* harbors one homologue of the *S. cerevisiae* ScRom1/ScRom2.** To identify homologues of ScRom1/ScRom2 in *A. fumigatus*, we performed a BLASTP search using the ScRom2 sequence and the genome database of *A. fumigatus* (25). The search resulted in only one homologue (AFUA_5G08550) with a length of 1,199 amino acids which has an identity and similarity of 28% and 41% with ScRom1 and 31% and 43% with ScRom2, respectively. We have named it AFUA_5G08550 Rom2. Closer analysis of Rom2 using InterProScan (26) revealed its conserved protein domains. As expected and similar to ScRom1/ScRom2, it contains a dishevelled, Egl-10, and pleckstrin (DEP) domain (PF00610), followed by a Rho GEF domain (PF00621) and a citron homology (CNH) domain (PF00780) from the N terminus to C terminus, respectively (Fig. 2A). A PFAM search (27) for proteins containing the Rho GEF domain (PF00621) in *A. fumigatus* listed six proteins, including Rom2. However, none of the other GEF domain proteins contained a DEP domain, and only one, AFUA_5G07430, harbored a CNH domain. AFUA_5G07430 is similar to the GEFs SpRgf3 (*S. pombe* Rgf3) and NcRGF3 (*N. crassa* RGF3) of *S. pombe* and *N. crassa*, respectively. SpRgf3 is a GEF of SpRho1 and controls β-(1,3)-D-glucan biosynthesis and cytokinesis (17, 18, 28), while NcRGF3 of the filamentous fungus *N. crassa* was shown to be a specific GEF of NcRHO4 and controls septum formation (29). In this study, we focused on analyzing Rom2.

Generation of a conditional *rom2* mutant. In *S. cerevisiae*, a strain with a double deletion of *ScROM1* and *ScROM2* is not viable. The same holds true for a double deletion of SpRgf1 and SpRgf2 in *Schizosaccharomyces pombe*. Despite repetitive attempts to generate a *rom2* gene deletion in *A. fumigatus*, we could not isolate a viable clone with the respective mutation. This suggested that *rom2* is an essential gene in *A. fumigatus*. We recently applied a doxycycline-inducible promoter to study the role of the essential gene *rho1*, a strategy that is suitable to obtain a rapid lethal effect under repression and growth like that of the wild type (wild-type-like growth) under induction (7). We therefore decided to construct a conditional *rom2* mutant ($rom2_{tetOn}$) by replacing the endogenous *rom2* promoter with a doxycycline-inducible promoter (Fig. 2B). As shown in Fig. 3A, the conditional *rom2* mutant was viable under repressive conditions on minimal medium. The addition of 0.25 to 0.5 μg/ml doxycycline reconstituted wild-type-like growth on solid medium, while the addition of higher doxycycline concentrations significantly repressed sporulation. Although the conditional *rom2* mutant was still viable in the absence of doxycycline, its radial growth was strikingly impaired and sporulation was completely abolished. Overexpression of *rom2* slightly reduced radial growth, and sporulation was significantly reduced compared to the wild type (Fig. 3B and D). We assumed that Rom2 is a GEF of Rho1 and expected that the over-

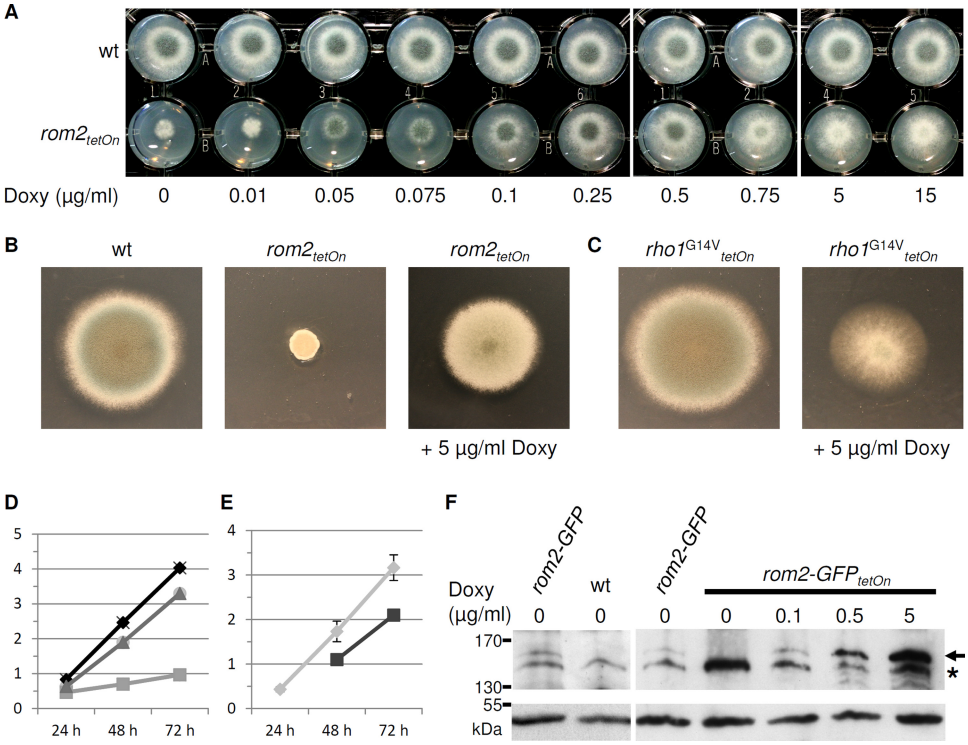

FIG 3 Doxycycline-dependent growth phenotypes of the conditional $rom2_{tetOn}$ mutant. (A to C) A total of 1.5×10^3 conidia of the indicated strains were spotted on AMM agar supplemented with the indicated amount of doxycycline (Doxy) and incubated for 36 h (A), 72 h (B), or 96 h (C) at 37°C. wt, wild type. (D and E) Mean radial growth diameters of strain AfS35 (black symbols and lines in panel D), $rom2_{tetOn}$ strain with 5 μg/ml doxycycline and without doxycycline (dark and light gray symbols and lines, respectively, in panel D), and $rho1^{G14V}{}_{tetOn}$ strain with 5 μg/ml doxycycline and without doxycycline (dark and light gray symbols and lines, respectively, in panel E) were measured after 24 h, 48 h, and 72 h. The *y* axis shows radial growth (in cm). Experiments were performed in triplicate, and error bars indicate the standard deviations only when they were large enough to visualize. (C and E) AMM agar was additionally supplemented with pyrithiamine to avoid loss of the $rho1^{G14V}{}_{tetOn}$ construct. (F) Conidia of the indicated strains were inoculated in AMM (10^6 conidia ml^{-1}) supplemented with the indicated amount of doxycycline and cultured at 37°C for 20 h. Protein extracts were analyzed by SDS-PAGE and Western blotting with antibodies directed against GFP (top panel) and Aspf22 (loading control; bottom panel). The arrow indicates Rom2-GFP. The asterisk indicates an unspecific band.

expression of *rom2* mimics the artificial constitutive activation of Rho1 (30). To test this hypothesis, we constructed a strain that expresses a constitutive active allele ($rho1^{G14V}{}_{tetOn}$) under a doxycycline-inducible promoter. The expression of the constitutive active $rho1^{G14V}$ resulted in a slightly reduced radial growth compared to the wild type. Sporulation was also drastically reduced, but the colony morphology appeared less compact compared to the strains overexpressing *rom2* (Fig. 3C and E).

Evaluation of *rom2* expression levels in the conditional *rom2* mutant. To assess *rom2* expression levels, we integrated the sequence for a C-terminal GFP tag at the endogenous *rom2* loci in the wild type and conditional $rom2_{tetOn}$ mutant. These strains, the *rom2-GFP* and $rom2\text{-}GFP_{tetOn}$ strains, were analyzed by fluorescence microscopy and Western blotting (Fig. 3F). Notably, growth and conidiation of the *rom2-GFP* and $rom2\text{-}GFP_{tetOn}$ strains were indistinguishable compared to the parental strains, suggesting that the GFP-tagged Rom2 is fully functional (data not shown). The endogenous Rom2-GFP levels in the *rom2-GFP* strain and in the noninduced or only weakly (0.1 μg/ml doxycycline) induced $rom2\text{-}GFP_{tetOn}$ strain were too low to detect with a conventional fluorescence microscope. Induction of the $rom2\text{-}GFP_{tetOn}$ gene in liquid cultures with 0.5 μg/ml doxycycline or more resulted in a weak but evident fluorescence (data not shown). Western blotting and immunodecoration with antibodies directed against GFP revealed a weak band at approximately 160 kDa in the *rom2-GFP* and induced $rom2\text{-}GFP_{tetOn}$ strains. As expected, Rom2-GFP was not detected in the parental wild type or noninduced $rom2\text{-}GFP_{tetOn}$ strain (Fig. 3F). Our results demonstrate that *rom2* expression driven by its endogenous promoter is rather low and that 0.1 μg/ml doxycycline is sufficient to induce wild-type-like expression levels in liquid medium.

Downregulation of *rom2* expression results in an increased susceptibility to cell wall-perturbing agents. In order to evaluate the importance of *rom2* for the CWI of *A. fumigatus*, we tested the sensitivity of the conditional *rom2* strain under repressed growth conditions to the cell wall-perturbing agents Congo red and calcofluor white. As shown in Fig. 4A, repression of *rom2* resulted in an increased sensitivity to these agents compared to the wild type. As expected, supplementing the medium with doxycycline reconstituted growth of the mutant. While the wild type can grow at high temperatures (>50°C), the repressed mutant strain showed a severe temperature sensitivity at 48°C. This growth defect was partially rescued by the addition of an osmotic stabilizer (1.2 M sorbitol), suggesting that the growth inhibition is associated with impaired CWI. In agreement with this hypothesis and in contrast to the wild type, the repressed $rom2_{tetOn}$ strain stained positive in a colorimetric phosphatase assay that indicates leakage of cytosol when exposed to elevated temperatures (Fig. 4B).

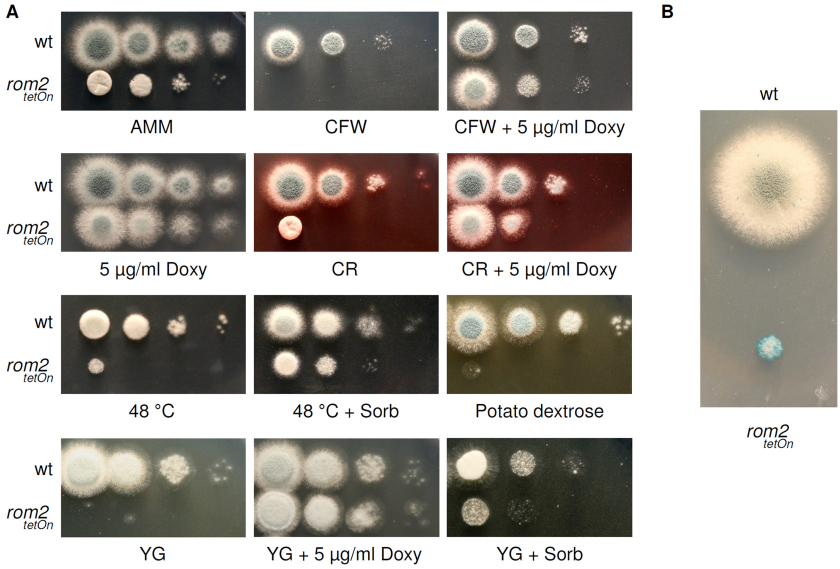

FIG 4 Reduced expression of *rom2* results in an increased susceptibility to cell wall-perturbing agents and heat associated with cytosolic leakage. (A) In a series of 10-fold dilutions derived from a starting suspension of 5×10^6 conidia ml^{-1} of the indicated strains, aliquots of 3 μl were spotted onto AMM agar or, when indicated, onto YG or potato dextrose agar. When indicated, AMM or YG was supplemented with Congo red (CR) (8 μg ml^{-1}), calcofluor white (CFW) (40 μg ml^{-1}), sorbitol (Sorb) (1.2 M), or doxycycline (Doxy). AMM agar plates were incubated at 37°C for 36 h or, when indicated, at 48°C for 48 h. YG and potato dextrose agar plates were incubated at 37°C for 24 h. (B) A total of 1.5×10^3 conidia were spotted on AMM agar and incubated at 37°C. After 36 h, the agar plates were shifted to 48°C. After 6 h of incubation at 48°C, the agar plates were overlaid with soft agar supplemented with 5-bromo-4-chloro-3-indolylphosphate and incubated for another 30 min at 48°C. Cell lysis (enzymatic activity) is visualized by blue coloring.

To our surprise, the conditional *rom2* mutant was not viable on complete media, e.g., YG or potato dextrose agar. Supplementing media with doxycycline completely reconstituted growth of the mutant. Supplementing the media with 1.2 M sorbitol partially rescued growth, suggesting that this growth phenotype is also associated with impaired CWI (Fig. 4A).

We have also tested the susceptibility of the repressed $rom2_{tetOn}$ mutant to other potentially cell wall-perturbing agents such as farnesol (1 mM), tunicamycin (10 μg ml^{-1}), and SDS (0.01% [wt/vol]). The $rom2_{tetOn}$ mutant showed an increased susceptibility to the detergent SDS, but not to farnesol or tunicamycin (data not shown).

Effects of repression or overexpression of *rom2* on hyphal growth and development. To analyze germination and hyphal growth, we cultured the conditional *rom2* mutant strain under induced and repressed conditions in liquid media suitable for microscopic examination. Repression of *rom2* resulted in delayed germination and growth compared to the wild type (data not shown). When shifting these swollen conidia and germ tubes to 48°C, they rapidly ruptured (Fig. 5A). As expected, induction with 0.5 μg/ml doxycycline resulted in wild-type-like growth and no cell lysis. Overexpression of *rom2* resulted in a growth delay combined with a hyperbranching phenotype when the strain was shifted to 48°C (Fig. 5A). This overexpression phenotype was not obvious in parallel cultures at standard growth temperature in the indicated time frame (37°C, 16 h; data not shown). We have previously shown that a mutant disrupted in the Bck1-Mkk2-MpkA MAP kinase module is less adherent to polar surfaces than the wild type (6). Notably, the adherence to polar surfaces of the repressed $rom2_{tetOn}$ strain was not reduced (data not shown). Expression of the constitutive active *rho1* gene with the G-to-V change at position 14 ($rho1^{G14V}$) did also significantly delay germination and growth, but this phenotype was already visible at 37°C and not associated with hyphal hyperbranching at elevated temperatures (Fig. 5B and data not shown).

Rom2 is required for caspofungin resistance but dispensable for resistance to azole antifungals. We and others have previously shown that the CWI pathway is involved in antifungal drug resistance. For example, disrupting the Bck1-Mkk2-MpkA MAP kinase module increases the sensitivity to azole antifungals and echinocandins (6, 14, 31). The stress sensor Wsc1, whose homologue in *S. cerevisiae* was shown to interact with ScRom2 (32), is specifically required for caspofungin resistance (14). On the other hand, no stress sensors with relevance to azole antifungal susceptibility were identified yet. We examined whether Rom2 is required for antifungal drug resistance using commercially available epsilometer test strips for posaconazole, voriconazole, and caspofungin. Repression of *rom2* resulted in a drastically increased caspofungin sensitivity (Fig. 6). However, the sensitivity to azoles was not increased (Fig. 6 and data not shown). Interestingly, overexpression of *rom2* did not affect, i.e., increase, the resistance of *A. fumigatus* to caspofungin (Fig. 6). In agreement with this finding, expression of $rho1^{G14V}$ also did not affect the caspofungin sensitivity (data not shown).

GFP-tagged Rom2 localizes to the cell membrane at the hyphal tips and to newly formed septa but is not required for septum formation. We have previously shown that a GFP-tagged Rho1 preferentially localizes to the hyphal tips (7). We assumed that Rom2 as the putative GEF and physical interaction partner of Rho1 would show a similar localization pattern. To visualize Rom2 in *Aspergillus*, we expressed a C-terminally GFP-tagged Rom2 ($rom2\text{-}GFP_{gpdA}$). Several GFP-positive clones were acquired, all showing reduced sporulation (overexpression phenotype of Rom2) and the same but very weak GFP pattern. Rom2-GFP clearly localized to the cell membrane and preferentially to

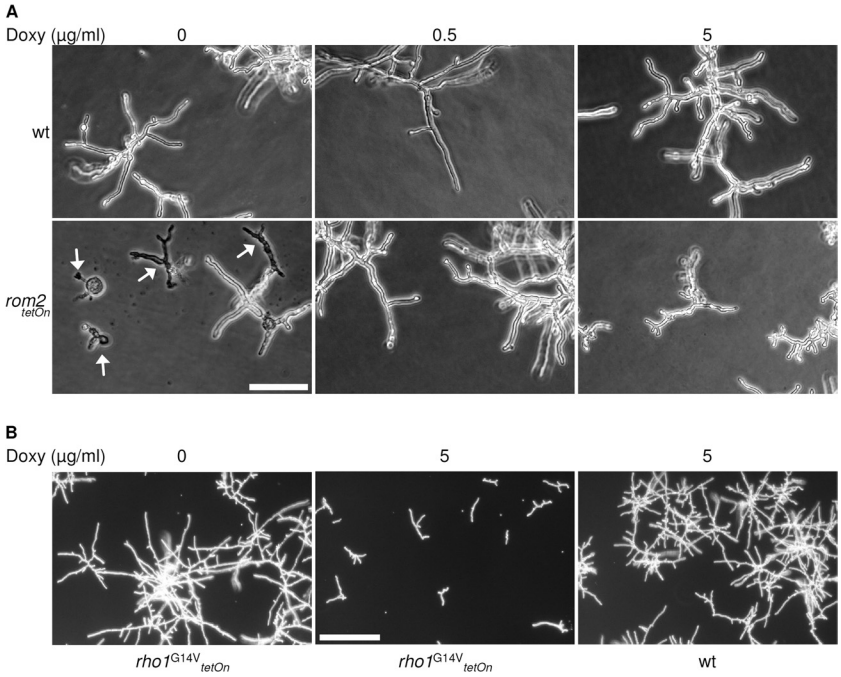

FIG 5 Abnormal germination and hyphal growth triggered by overexpression or repression of *rom2* or expression of a dominant active *rho1* allele. (A and B) A total of 5×10^3 conidia ml^{-1} of the indicated strains were inoculated in the wells on plates in liquid AMM supplemented with 0, 0.5, or 5 μg ml^{-1} doxycycline (Doxy). (A) The plates were incubated at 37°C for 12 h and then shifted to 48°C for 4 h. Bar, 100 μm. (B) The plates were incubated at 37°C for 16 h. Bar, 250 μm.

hyphal tips (Fig. 7A). Interestingly, we also found Rom2-GFP concentrated at the sites of newly formed septa (Fig. 7B), suggesting a role in septum formation. We therefore examined the presence of septa in the hyphae of the $rom2_{tetOn}$ strain, but the $rom2_{tetOn}$ strain was still able to form multiple septa under repressive conditions (data not shown).

Repression of *rom2* results in a reduced inducibility but increased basal activity of MpkA. In *A. fumigatus*, the MAP kinase

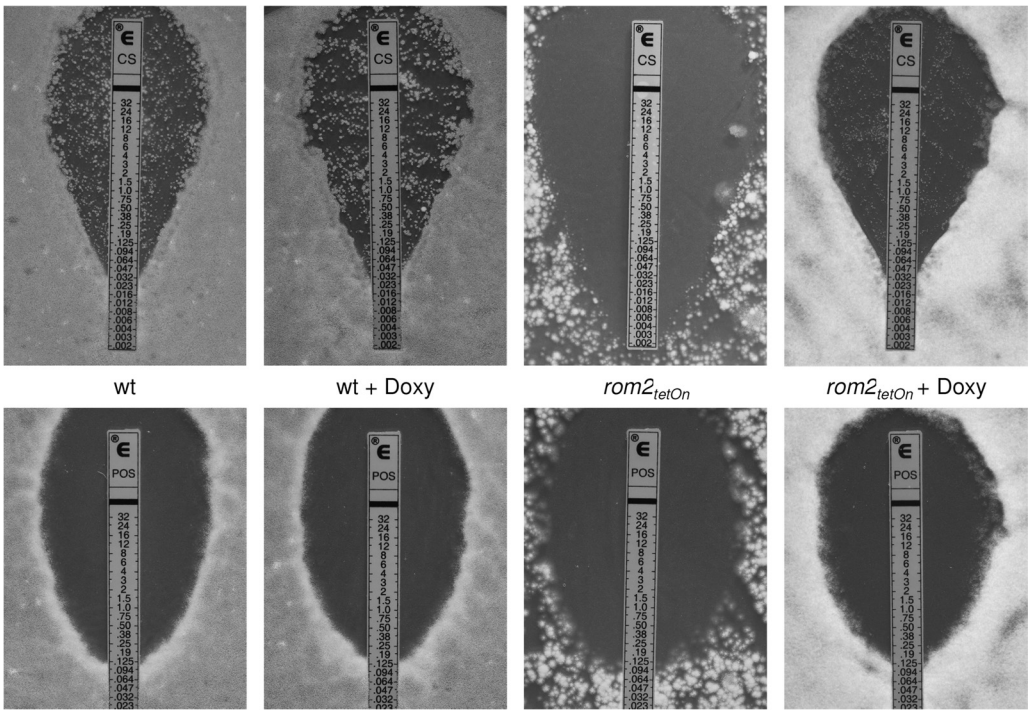

FIG 6 Rom2 is required for echinocandin tolerance. A total of 2.5×10^4 conidia of the indicated strains were spread on AMM agar plates. When indicated, AMM was supplemented with 5 μg ml^{-1} doxycycline (Doxy). Caspofungin (top panels) or posaconazole (bottom panels) Etest strips were applied, and the agar plates were incubated at 37°C. Representative photos were taken after 48 h.

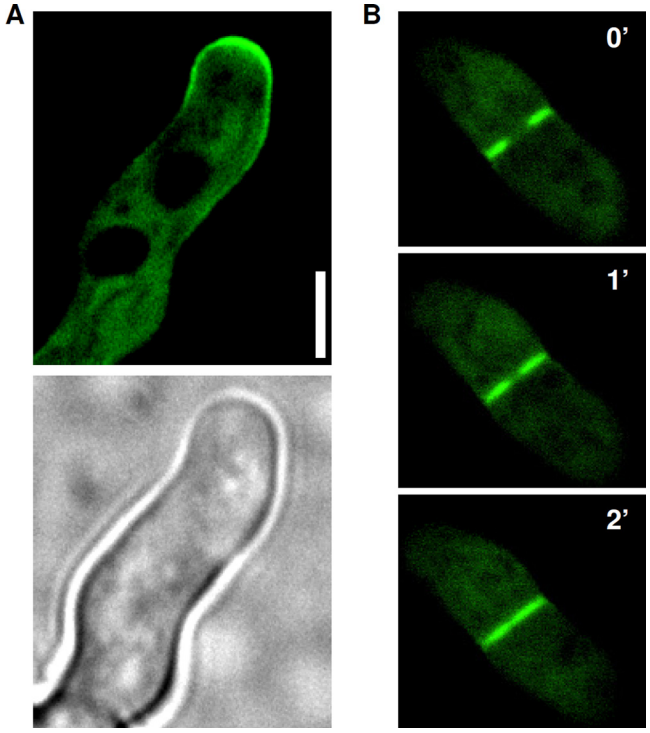

FIG 7 GFP-tagged Rom2 localizes to the hyphal tips and septa. (A and B) Conidia of a wild-type strain expressing a C-terminally GFP-tagged Rom2 were inoculated in AMM and cultured at 37°C for approximately 15 h. Fluorescence (top panel of panel A and all panels in panel B) and bright-field (bottom panel in panel A) images were taken with a spinning disc confocal microscope and represent one optical section of living hyphae. (B) The time lapse pictures of the forming septum were taken after 0, 1, and 2 min as indicated. Bar, 5 μm.

MpkA is phosphorylated under cell wall stress (6, 7, 9, 31). The same applies to the homologous MAP kinases in *S. cerevisiae* and other fungal species (33, 34). We recently showed that the calcofluor white-induced phosphorylation of the MAP kinase MpkA of *A. fumigatus* is reduced in a mutant lacking MidA, which is in agreement with its proposed function as a stress sensor (14). We investigated the basal and induced phosphorylation of MpkA in the *rom2*$_{tetOn}$ strain under repressive growth conditions. As shown in Fig. 8, the basal phosphorylation of MpkA was significantly increased in the conditional *rom2* mutant under repressive conditions compared to the wild type. In the wild type, exposure to the cell wall stressor calcofluor white induces a striking phosphorylation of MpkA, whereas the high basal phosphorylation of MpkA in the *rom2*$_{tetOn}$ strain under repressive conditions is not further enhanced by calcofluor white (Fig. 8).

We have also noticed a calcofluor white-induced phosphorylation of MpkB in the wild type. This is in line with our previous observation that MpkB may also be activated through cell wall stress (6). Interestingly, this stress-induced phosphorylation of MpkB also occurs in the *rom2*$_{tetOn}$ strain under repressive growth conditions and is enhanced under calcofluor white-induced stress (Fig. 8).

Expression of an N-terminally truncated Rom2. When the present study was initiated, the relevance of the DEP domain present in Rom2 and its homologues in other species was unknown. Very recently, the research group of Stephan Seiler showed that the DEP domain of NcRGF1, a Rom2 homologue in *Neurospora crassa* that acts as a specific GEF for NcRHO1, negatively self-regulates its GEF activity (16). We speculated that a similar self-inhibitory mechanism could also exist in Rom2. If the DEP domain of Rom2 has an autoinhibitory effect, the overexpression of Rom2(733-1199) that lacks the N-terminal region with the DEP domain should have more drastic effects on fungal growth and development than the overexpression of the full-length protein. Two mutants were generated, either ectopically expressing the full-length protein (C-terminally His tagged) or an N-terminally HA-tagged Rom2(733-1199) under a doxycycline-inducible promoter. As expected and as shown in Fig. 9A, ectopic overexpression of the full-length protein resulted in a moderate growth phenotype that copies the phenotype of the conditional *rom2*$_{tetOn}$ strain cultured under similar conditions, i.e., strikingly reduced sporulation and slightly reduced radial growth. In contrast, overexpression of HA-Rom2(733-1199) resulted in a significantly stronger growth phenotype: radial growth was drastically reduced, and no sporulation was detected. Overexpression of Rom2(733-1199) also had drastic effects on germination and hyphal growth compared to overexpression of full-length Rom2 in liquid media (Fig. 9B). Notably, increasing the doxycyline supplementation of the medium by a factor of 10 (50 μg ml^{-1}) did not significantly

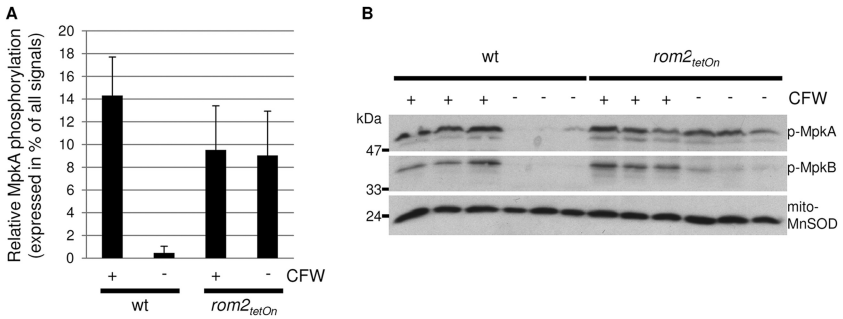

FIG 8 Reduced expression of *rom2* results in an increased basal and less stress-induced phosphorylation of MpkA. (A and B) Conidia of the wild type (wt) and *rom2*$_{tetOn}$ strain were inoculated in triplicate in AMM (10^5 conidia ml^{-1}) and cultured at 37°C in a tube rotator. After 24 h, calcofluor white (CFW) (100 μg ml^{-1}) was added (+) or not added (−) to each sample and incubated for 30 min. Protein extracts were analyzed by SDS-PAGE and Western blotting with anti-phospho-p44/42 MAPK antibodies directed against phosphorylated MpkA (p-MpkA) and phosphorylated MpkB (p-MpkB). The relative quantity of phosphorylated MpkA expressed as a percentage of all signals is given in panel A. Error bars indicated the standard deviations of three replicate samples. Antibodies directed against the mitochondrial MnSOD were used for a loading control (bottom panel in panel B).

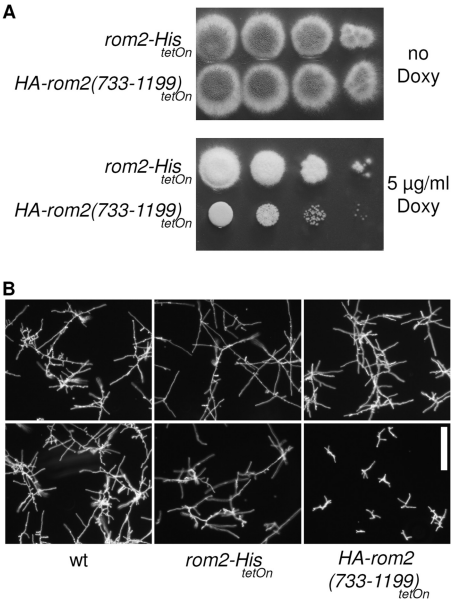

FIG 9 HA-Rom2(733-1199) induces a different growth phenotype than the full-length protein. (A) In a series of 10-fold dilutions derived from a starting suspension of 5×10^6 conidia ml^{-1} of the indicated strains, aliquots of 3 μl were spotted onto AMM supplemented with the indicated amount of doxycycline (Doxy) and incubated for 48 h at 37°C. AMM agar was additionally supplemented with hygromycin B to avoid loss of the respective construct. (B) A total of 5×10^3 conidia ml^{-1} of the indicated strains were inoculated in the wells on plates in liquid AMM supplemented with no doxycycline (top panels) or 5 μg ml^{-1} doxycycline (bottom panels). The plates were incubated at 37°C for 16 h. Bar, 250 μm.

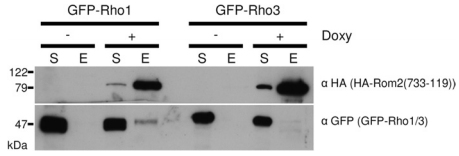

FIG 10 HA-Rom2(733-1199) interacts with GFP-Rho1. Coimmunoprecipitation of HA-Rom2(733-1199) and GFP-tagged Rho1. Conidia of strains constitutively expressing GFP-Rho1 or GFP-Rho3 and conditionally expressing HA-Rom2(733-1199) were inoculated in AMM and incubated on a rotary shaker at 37°C. After 24 h, HA-Rom2(733-1199) expression was induced with 50 μg ml^{-1} doxycycline (+) or not induced with doxycycline (−), and the cultures were incubated for another 4 h at 37°C. The soluble fractions (S) of mycelium extracts were subjected to anti-HA agarose. After two wash steps, bound protein was eluted (E). Portions (0.125%) of the soluble fraction (S) and 30% of the elution (E) were analyzed by SDS-PAGE and Western blotting with anti-HA antibodies (α HA) and anti-GFP antibodies (α GFP).

enhance the overexpression phenotypes of full-length Rom2 or Rom2(733-1199), suggesting that the expression of both constructs is maximally induced. Although we cannot fully exclude the possibility that other effects might alter the abundance or activity of full-length Rom2 and Rom2(733-1199) differently, e.g., posttranscriptional regulation, these data support a model where the N-terminal region of Rom2 (amino acids 1 to 732) negatively regulates its activity.

Rom2 interacts with Rho1. To investigate the potential interaction of Rom2 and Rho1, we performed coimmunoprecipitations. HA-Rom2(733-1199) appears to be more active than the full-length Rom2 protein. Therefore, we decided to use the more active C-terminal Rom2 fragment that includes the Rho GEF domain to perform the pulldown experiments. *A. fumigatus* strains constitutively expressing GFP-tagged Rho1 or Rho3, which show very similar subcellular localization patterns (7), were transformed with a doxycycline-inducible construct for the ectopic expression of an N-terminally HA-tagged Rom2(733-1199). As shown in Fig. 10, GFP-Rho1, but not GFP-Rho3, coimmunoprecipitated with HA-Rom2(733-1199) if the strain was exposed to doxycycline for 4 h. In the absence of doxycycline, HA-Rom2(733-1199) was not expressed, and thus, GFP-Rho1 was not coimmunoprecipitated.

DISCUSSION

Recently, we functionally characterized *A. fumigatus* cell wall stress sensors (Wsc1, Wsc3, and MidA) and Rho GTPases with implications for the CWI (14). According to a model derived from data in yeast, the sensors would signal to the respective downstream Rho GTPase with the help of a Rho GEF. If Rom2 were to function as such an essential, integrating, and nonredundant GEF, one would expect a combination of the phenotypes we have previously found for the sensors.

In fact, we found that the $rom2_{tetOn}$ mutant under repressive conditions shares several phenotypes with the deletion mutants of the three CWI sensors. We have shown that downregulation of *rom2* results in a striking sensitivity to the β-(1,3)-D-glucan synthesis inhibitor caspofungin. While MidA and Wsc3 are dispensable for resisting echinocandins, a deletion of *wsc1* results in a significantly decreased MIC of caspofungin (14). Repression of *rom2* does also result in a striking sensitivity to the chitin binding and cell wall-perturbing agents Congo red and calcofluor white. In addition, we observed an increased temperature sensitivity which was partially remediated by osmotic stabilization of the medium. Here, Wsc1 and Wsc3 are dispensable, but MidA shows a very similar sensitivity to Congo red, calcofluor white, and heat. In agreement with a role of MidA as a stress sensor, the calcofluor white-induced MpkA phosphorylation is reduced in a mutant lacking *midA* (14). Similarly, we could not further boost the basal MpkA phosphorylation levels with calcofluor white in the repressed $rom2_{tetOn}$ mutant. Finally, reduced *rom2* expression results in drastically reduced radial growth and sporulation. Notably, none of the single deletions of *wsc1*, *wsc3*, or *midA* results in a significantly impaired radial growth of the respective mutants. On the other hand, radial growth and sporulation of a Δ*wsc1* Δ*wsc3* double mutant were slightly reduced, and radial growth and sporulation of a Δ*wsc1* Δ*wsc3* Δ*midA* triple mutant were drastically reduced (14). This underlines the partially overlapping roles of the three sensors and is perfectly in line with a model where Rom2 functions as the major and nonredundant relay molecule for stress signals of these three CWI sensors in *A. fumigatus*.

The $rom2_{tetOn}$ mutant cultured under repressive growth conditions shows increased basal MpkA phosphorylation levels compared to the wild type. At a first glance, this is surprising, since one could expect reduced MpkA phosphorylation levels if a major upstream activator were eliminated. However, these data are in good agreement with similar observations in yeast and, very recently, in the filamentous fungus *N. crassa*. In *S. cerevisiae*, deletion of *ScROM2* results in an increased basal phosphorylation of ScMpk1 (35). In *N. crassa*, a heterokaryon deletion of *Ncrgf-1* also results in an increased basal phosphorylation of the MpkA homologue NcMAK1 (16). According to our results and on the basis of similar observations made in other fungi, we propose that alter-

native stress signaling mechanisms can activate the downstream Bck1-Mkk2-MpkA CWI MAP kinase module independently of Rom2 in mutants with chronic cell wall stress.

Three of six *Aspergillus* Rho GTPases are important for the integrity of the cell wall, but the respective involvement in the CWI signaling process was not clear. Notably, of the three Rho GTPases, only Rho1 is essential in *Aspergillus*, and while the Δ*rho2* mutant shows no remarkable growth abnormality under standard growth conditions, lack of Rho4 results in only a moderately affected growth phenotype (reduced sporulation and slightly reduced radial growth) (13, 14). Our data indicate that Rho1 is the primary relevant Rho GTPase in CWI signaling. First, reduced *rom2* expression results in drastically altered growth with the absence of sporulation and radial growth on minimal media (AMM), and on complete media, the repressed mutant is not viable due to cell lysis during germination. This growth failure best correlates with the essential function of Rho1 and not with the role of Rho2 or Rho4. Second, we were able to pull down Rho1, but not Rho3, which shows a similar subcellular localization (7), with Rom2 in *A. fumigatus*, thereby strongly suggesting a specific interaction of these two proteins.

Some of our data could argue for an interaction of Rom2 and Rho4. Previously, we found that the deletion of *rho4*, but not of *rho2*, results in an increased susceptibility to caspofungin in *A. fumigatus* which is similar to a lack of Rom2 function (14). Also, in the present work, we showed that GFP-tagged Rom2 localizes to newly formed septa, a localization pattern which is specific for Rho4. The only currently known cellular function of Rho4 in *Aspergillus* is its essentiality for septum formation (13, 14, 36). Thus, our data could point either to an additional involvement of Rho4 in CWI signaling or to an involvement of Rom2 in the septum formation process. We think it is less likely that Rho4 has a prominent role in CWI signaling, since the calcofluor white-induced MpkA phosphorylation is not reduced in the mutant (14). Instead, the susceptibility of the Δ*rho4* mutant to caspofungin could be a consequence of the absent septum formation. Echinocandins provoke rupturing and cytosolic leakage of hyphal tips in *A. fumigatus*. This is usually not fatal for the wild type, since it occurs only occasionally and never affects the whole microcolony, even with high doses of echinocandins (37). It is conceivable that a mutant lacking the septa that compartmentalize the hyphae is much more vulnerable to occasional hyphal tip rupturing and cytosolic leakage.

Notably, GEFs of the respective Rho4 homologues have already been identified and characterized in other filamentous fungi. In *A. nidulans*, *A. nidulans* Bud3 (AnBud3) is a GEF of AnRho4 and essential for septum formation (36), and in *N. crassa*, even two nonredundant GEFs of NcRHO4 were identified, NcBUD3 and NcRGF3 (29). NcRGF3 is the homologue of AFUA_5G07430 which has a domain structure similar to Rom2 but is currently uncharacterized in *Aspergillus*. Since the $rom2_{tetOn}$ strain still forms multiple septa under repressive growth conditions, a GEF activity of Rom2 on Rho4 remains speculative and is, at the most, redundant or supportive of the other two likely Rho4 GEFs Bud3 (AFUA_5G11890) and AFUA_5G07430. We cannot exclude the possibility that GFP-tagged Rom2 mislocalizes to septa due to overexpression. On the other hand, this localization may also reflect a potential role of Rho1 during septum formation, which is evident in *S. cerevisiae* and *S. pombe* (3, 17). The Rom2-GFP localization to the hyphal tips is in good agreement with the recently characterized subcellular localization pattern of its homologue NcRGF1 in *N. crassa* and the predominant localization of its interacting Rho GTPase Rho1 to the hyphal tips (7, 16).

Very recently, Richthammer et al. analyzed the essential role of the Rho1 homologue NcRHO1 in *N. crassa*. They have shown that the GEF domain of the Rom2 homologue NcRGF1 can promote GDP-GTP exchange only at NcRHO1 and not at any other *N. crassa* Rho GTPase *in vitro* (16). Jointly with our data, it appears that the Rho GTPase specificity of ScRom1/ScRom2 homologues is generally conserved from yeasts to filamentous fungi.

An interesting finding of Richthammer et al. is the autoinhibitory function of the DEP domain within the N-terminal part of NcRGF1. DEP domains are known to facilitate protein-protein interactions, for example in the context of G-protein-coupled receptor signaling in yeast (38). Richthammer et al. observed that *in vitro* the GEF domain of NcRGF1 can induce only GDP-GTP exchange at NcRHO1 if the DEP domain is not included in the construct. According to their proposed model which is supported by yeast two-hybrid data, NcRGF1 interacts with its N-terminal region with a Wsc1-like putative stress sensor of *N. crassa*. This relieves the autoinhibitory effect of the DEP domain and allows activation of NcRHO1 through GDP-GTP exchange (16). We have shown that the expression of a C-terminal Rom2 portion that lacks the N terminus and DEP domain but includes the GEF domain induces a strikingly stronger growth phenotype than the expression of the full-length protein alone. Our results suggest that the model of Richthammer et al. also applies to *A. fumigatus*.

The fungal cell wall, an essential structure not present in mammals, and the underlying CWI pathway remain attractive drug targets for antifungal therapy. Our work demonstrated the crucial role of Rom2 in the cell wall stress tolerance of *A. fumigatus*. The importance of Rom2 in echinocandin resistance is particularly relevant and functionally links it to its putative upstream activator, Wsc1. It will be interesting to understand the nature of the increased echinocandin sensitivity we have observed in the Δ*wsc1* mutant and conditional *rom2* mutants. New insights could promote future efforts in optimizing the effectiveness of these clinically highly relevant drugs.

ACKNOWLEDGMENTS

We thank Emilia Sieger for excellent technical assistance. We thank Frank Ebel for critically reading the manuscript.

This work was supported by the "Förderprogramm für Forschung und Lehre" of the Ludwig-Maximilians-Universität, the Münchner Medizinische Wochenschrift, and the Deutsche Forschungsgemeinschaft (WA3016/1-1).

REFERENCES

1. **Fontaine T, Simenel C, Dubreucq G, Adam O, Delepierre M, Lemoine J, Vorgias CE, Diaquin M, Latgé JP.** 2000. Molecular organization of the alkali-insoluble fraction of *Aspergillus fumigatus* cell wall. J. Biol. Chem. **275**:27594–27607.
2. **Levin DE.** 2011. Regulation of cell wall biogenesis in *Saccharomyces cerevisiae*: the cell wall integrity signaling pathway. Genetics **189**:1145–1175.
3. **Perez P, Rincón SA.** 2010. Rho GTPases: regulation of cell polarity and growth in yeasts. Biochem. J. **426**:243–253.
4. **Rodicio R, Buchwald U, Schmitz H-P, Heinisch JJ.** 2008. Dissecting sensor functions in cell wall integrity signaling in *Kluyveromyces lactis*. Fungal Genet. Biol. **45**:422–435.
5. **Sekiya-Kawasaki M, Abe M, Saka A, Watanabe D, Kono K, Minemura-Asakawa M, Ishihara S, Watanabe T, Ohya Y.** 2002. Dissection of upstream regulatory components of the Rho1p effector, 1,3-beta-glucan synthase, in *Saccharomyces cerevisiae*. Genetics **162**:663–676.

6. **Dirr F, Echtenacher B, Heesemann J, Hoffmann P, Ebel F, Wagener J.** 2010. AfMkk2 is required for cell wall integrity signaling, adhesion, and full virulence of the human pathogen *Aspergillus fumigatus*. Int. J. Med. Microbiol. **300**:496–502.
7. **Dichtl K, Ebel F, Dirr F, Routier FH, Heesemann J, Wagener J.** 2010. Farnesol misplaces tip-localized Rho proteins and inhibits cell wall integrity signalling in *Aspergillus fumigatus*. Mol. Microbiol. **76**:1191–1204.
8. **Valiante V, Jain R, Heinekamp T, Brakhage AA.** 2009. The MpkA MAP kinase module regulates cell wall integrity signaling and pyomelanin formation in *Aspergillus fumigatus*. Fungal Genet. Biol. **46**:909–918.
9. **Valiante V, Heinekamp T, Jain R, Härtl A, Brakhage AA.** 2008. The mitogen-activated protein kinase MpkA of *Aspergillus fumigatus* regulates cell wall signaling and oxidative stress response. Fungal Genet. Biol. **45**: 618–627.
10. **Ichinomiya M, Uchida H, Koshi Y, Ohta A, Horiuchi H.** 2007. A protein kinase C-encoding gene, *pkcA*, is essential to the viability of the filamentous fungus *Aspergillus nidulans*. Biosci. Biotechnol. Biochem. **71**:2787–2799.
11. **Ronen R, Sharon H, Levdansky E, Romano J, Shadkchan Y, Osherov N.** 2007. The *Aspergillus nidulans pkcA* gene is involved in polarized growth, morphogenesis and maintenance of cell wall integrity. Curr. Genet. **51**: 321–329.
12. **Teepe AG, Loprete DM, He Z, Hoggard TA, Hill TW.** 2007. The protein kinase C orthologue PkcA plays a role in cell wall integrity and polarized growth in *Aspergillus nidulans*. Fungal Genet. Biol. **44**:554–562.
13. **Kwon MJ, Arentshorst M, Roos ED, van den Hondel CAMJJ, Meyer V, Ram AFJ.** 2011. Functional characterization of Rho GTPases in *Aspergillus niger* uncovers conserved and diverged roles of Rho proteins within filamentous fungi. Mol. Microbiol. **79**:1151–1167.
14. **Dichtl K, Helmschrott C, Dirr F, Wagener J.** 2012. Deciphering cell wall integrity signalling in *Aspergillus fumigatus*: identification and functional characterization of cell wall stress sensors and relevant Rho GTPases. Mol. Microbiol. **83**:506–519.
15. **Maddi A, Dettman A, Fu C, Seiler S, Free SJ.** 2012. WSC-1 and HAM-7 are MAK-1 MAP kinase pathway sensors required for cell wall integrity and hyphal fusion in *Neurospora crassa*. PLoS One **7**:e42374. doi:10.1371/journal.pone.0042374.
16. **Richthammer C, Enseleit M, Sanchez-Leon E, März S, Heilig Y, Riquelme M, Seiler S.** 2012. RHO1 and RHO2 share partially overlapping functions in the regulation of cell wall integrity and hyphal polarity in *Neurospora crassa*. Mol. Microbiol. **85**:716–733.
17. **Mutoh T, Nakano K, Mabuchi I.** 2005. Rho1-GEFs Rgf1 and Rgf2 are involved in formation of cell wall and septum, while Rgf3 is involved in cytokinesis in fission yeast. Genes Cells **10**:1189–1202.
18. **Morrell-Falvey JL, Ren L, Feoktistova A, Haese GD, Gould KL.** 2005. Cell wall remodeling at the fission yeast cell division site requires the Rho-GEF Rgf3p. J. Cell Sci. **118**:5563–5573.
19. **García P, García I, Marcos F, de Garibay GR, Sánchez Y.** 2009. Fission yeast rgf2p is a rho1p guanine nucleotide exchange factor required for spore wall maturation and for the maintenance of cell integrity in the absence of rgf1p. Genetics **181**:1321–1334.
20. **Hill TW, Kafer E.** 2001. Improved protocols for *Aspergillus* minimal medium: trace element and minimal medium salt stock solutions. Fungal Genetics Newsl. **48**:20–21.
21. **Krappmann S, Sasse C, Braus GH.** 2006. Gene targeting in *Aspergillus fumigatus* by homologous recombination is facilitated in a nonhomologous end-joining-deficient genetic background. Eukaryot. Cell **5**:212–215.
22. **Meyer V, Wanka F, van Gent J, Arentshorst M, van den Hondel CAMJJ, Ram AFJ.** 2011. Fungal gene expression on demand: an inducible, tunable, and metabolism-independent expression system for *Aspergillus niger*. Appl. Environ. Microbiol. **77**:2975–2983.
23. **Wagener J, Echtenacher B, Rohde M, Kotz A, Krappmann S, Heesemann J, Ebel F.** 2008. The putative alpha-1,2-mannosyltransferase AfMnt1 of the opportunistic fungal pathogen *Aspergillus fumigatus* is required for cell wall stability and full virulence. Eukaryot. Cell **7**:1661–1673.
24. **Cabib E, Duran A.** 1975. Simple and sensitive procedure for screening yeast mutants that lyse at nonpermissive temperatures. J. Bacteriol. **124**: 1604–1606.
25. **Arnaud MB, Chibucos MC, Costanzo MC, Crabtree J, Inglis DO, Lotia A, Orvis J, Shah P, Skrzypek MS, Binkley G, Miyasato SR, Wortman JR, Sherlock G.** 2010. The *Aspergillus* Genome Database, a curated comparative genomics resource for gene, protein and sequence information for the *Aspergillus* research community. Nucleic Acids Res. **38**:D420–D427.
26. **Zdobnov EM, Apweiler R.** 2001. InterProScan–an integration platform for the signature-recognition methods in InterPro. Bioinformatics **17**: 847–848.
27. **Finn RD, Mistry J, Tate J, Coggill P, Heger A, Pollington JE, Gavin OL, Gunasekaran P, Ceric G, Forslund K, Holm L, Sonnhammer ELL, Eddy SR, Bateman A.** 2010. The Pfam protein families database. Nucleic Acids Res. **38**:D211–D222.
28. **Tajadura V, García B, García I, García P, Sánchez Y.** 2004. *Schizosaccharomyces pombe* Rgf3p is a specific Rho1 GEF that regulates cell wall beta-glucan biosynthesis through the GTPase Rho1p. J. Cell Sci. **117**: 6163–6174.
29. **Justa-Schuch D, Heilig Y, Richthammer C, Seiler S.** 2010. Septum formation is regulated by the RHO4-specific exchange factors BUD3 and RGF3 and by the landmark protein BUD4 in *Neurospora crassa*. Mol. Microbiol. **76**:220–235.
30. **Guest GM, Lin X, Momany M.** 2004. *Aspergillus nidulans* RhoA is involved in polar growth, branching, and cell wall synthesis. Fungal Genet. Biol. **41**:13–22.
31. **Fujioka T, Mizutani O, Furukawa K, Sato N, Yoshimi A, Yamagata Y, Nakajima T, Abe K.** 2007. MpkA-dependent and -independent cell wall integrity signaling in *Aspergillus nidulans*. Eukaryot. Cell **6**:1497–1510.
32. **Philip B, Levin DE.** 2001. Wsc1 and Mid2 are cell surface sensors for cell wall integrity signaling that act through Rom2, a guanine nucleotide exchange factor for Rho1. Mol. Cell. Biol. **21**:271–280.
33. **Martín H, Rodríguez-Pachón JM, Ruiz C, Nombela C, Molina M.** 2000. Regulatory mechanisms for modulation of signaling through the cell integrity Slt2-mediated pathway in *Saccharomyces cerevisiae*. J. Biol. Chem. **275**:1511–1519.
34. **Madrid M, Soto T, Khong HK, Franco A, Vicente J, Pérez P, Gacto M, Cansado J.** 2006. Stress-induced response, localization, and regulation of the Pmk1 cell integrity pathway in *Schizosaccharomyces pombe*. J. Biol. Chem. **281**:2033–2043.
35. **Lorberg A, Jacoby JJ, Schmitz HP, Heinisch JJ.** 2001. The PH domain of the yeast GEF Rom2p serves an essential function in vivo. Mol. Genet. Genomics **266**:505–513.
36. **Si H, Justa-Schuch D, Seiler S, Harris SD.** 2010. Regulation of septum formation by the Bud3-Rho4 GTPase module in *Aspergillus nidulans*. Genetics **185**:165–176.
37. **Ingham CJ, Schneeberger PM.** 2012. Microcolony imaging of *Aspergillus fumigatus* treated with echinocandins reveals both fungistatic and fungicidal activities. PLoS One **7**:e35478. doi:10.1371/journal.pone.0035478.
38. **Ballon DR, Flanary PL, Gladue DP, Konopka JB, Dohlman HG, Thorner J.** 2006. DEP-domain-mediated regulation of GPCR signaling responses. Cell **126**:1079–1093.